

## DIFFERENTIAL SCANNING CALORIMETRY OF EPOXY CURE: ISOTHERMAL CURE KINETICS\*

S. SOUROUR\*\* AND M. R. KAMAL

*Department of Chemical Engineering, McGill University, Montreal, Quebec (Canada)*

### ABSTRACT

The curing reactions of diglycidyl ether of bisphenol A with *m*-phenylene diamine (*m*-PDA) were studied with a differential scanning calorimeter (DSC) under isothermal conditions in the range 50–150°C. A computerized data acquisition system was used to collect and process rate and integral heat of reaction data during cure. A mathematical model describing the auto-accelerated reactions up to the diffusion-controlled stage is proposed. The rate constants were determined and used in the model to predict the progress of the cure reaction at different temperatures. Agreement with experimental reaction rate data is within  $\pm 5\%$ . The activation energies for these rate constants are 11–18 kcal mol<sup>-1</sup>. Overall activation energies determined from rheological gel time measurements and predicted gel time from the kinetic model are 11–12 kcal mol<sup>-1</sup>. The rate of heat generation at the peak of the reaction isotherm curve was correlated with the isothermal cure temperature using an Arrhenius equation. The extent of conversion at the peak was found constant and was used to obtain heat of cure at high temperatures. Values for the overall activation energy calculated from the gel time and the peak reaction rate are 11–12 kcal mol<sup>-1</sup>. The residual conversion after an isothermal cure at temperature  $T_c$ , varied exponentially with the glass transition temperature  $T_g$ . The latter was found to be 10–13°C higher than  $T_c$ . The  $T_g$  of the fully cured material is 122–158°C depending on the amount of diamine used. The isothermal cure temperature below which the material passes through vitrification without gelling was determined from DSC cure data. The results presented in this paper are discussed and compared with published data.

### INTRODUCTION

The physical, mechanical, and electrical properties of a thermosetting polymer depend to a large extent on the degree of cure. On the other hand, the processability of a thermoset resin critically depends on the rate and extent of polymerization under process conditions. Therefore, kinetic characterization of the reactive resin is not only important for a better understanding of structure-property relationships, but it is also fundamental in optimizing process conditions and product quality.

\*Presented at the 5th North American Thermal Society Meeting, Peterborough, Ontario, Canada, June 8–14, 1975.

\*\*Present address: DuPont of Canada Ltd., Research Center, P.O. Box 5000, Kingston, Ontario, Canada.

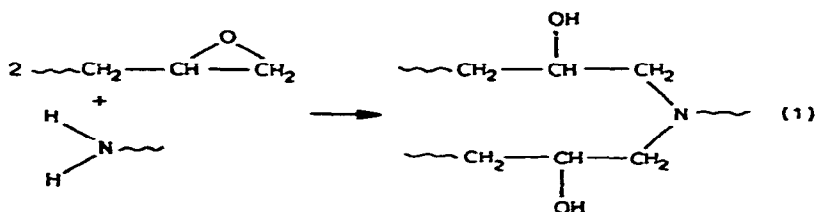
A number of experimental techniques and studies relating to thermosetting cure reactions have been reported in the literature with emphasis on the chemical, physical, and mechanical property changes with time<sup>1-6</sup>. Changes in physical properties such as refractive index<sup>7</sup>, electrical resistivity<sup>8-11</sup>, and density<sup>12,13</sup> have been used to determine the relative extent of cure in epoxy resins systems. In addition to chemical analysis<sup>14-16</sup>, infrared spectroscopy<sup>2,17,18</sup> has also been applied to determine the rate of cure of epoxy resins. Changes in viscosity<sup>14,18,19</sup> and gel point measurements<sup>18-26</sup> have been used to study the kinetics of the cure reactions. Dynamic mechanical techniques<sup>12,25-31</sup> such as torsional braid analysis (TBA) have been employed to follow the progress of the crosslinking reactions under isothermal and non-isothermal conditions, throughout the liquid-to-solid transition.

Differential scanning calorimetry (DSC) was used by a number of workers<sup>10,31-36</sup> to study the cure kinetics of epoxy resins. Kinetic parameters were determined from dynamic and isothermal DSC data with the assumption that the exothermic heat evolved during cure is proportional to the extent of monomer conversion<sup>37-41</sup>. With a few exceptions, the isothermal reaction rate—which was found to be autocatalytic<sup>33</sup>—has been described by an  $n$ th order kinetic expression with an overall Arrhenius rate constant fitted to the data. Values of  $n$  varied from 0.5 to 2.1 depending on temperature<sup>10</sup>. No comparison between predicted and experimental cure data was made to verify the validity and consistency of that model which in fact was misused in some cases to predict kinetic parameters from dynamic DSC cure data.

The purpose of this work is to analyze the cure kinetics of typical epoxy/aromatic diamine systems using DSC. These systems were chosen because they are typically reactive prepolymers and are commercially important. Isothermal DSC and rheological (viscosity-time) data were used to establish the validity of a kinetic model proposed to describe the progress of the cure reaction under isothermal conditions. The results are discussed with respect to those reported in the literature.

#### THEORY

It is well known that the uncatalyzed reaction of an epoxide with a primary amine produces a secondary amine which reacts with another epoxy group to form a tertiary amine. These reactions are auto-accelerated by the hydroxyl groups formed in the reactions<sup>16,20,33</sup>. Shechter<sup>16</sup> showed that the exclusive reaction was that of amine with epoxide and no evidence for etherification was found. Also there was no great selectivity in the reaction of a primary amine with a glycidyl ether successively from secondary to tertiary amine



The reactions are initiated by any hydrogen-bond donor molecules HX (e.g., moisture, impurities). These together with the hydroxyl groups act as true catalysts and are not consumed in any side-reactions. The concentration of hydroxyl groups continuously changes during the reaction while the concentration of the HX molecules remains constant. If it is assumed that the amine hydrogen atoms have equal reactivity<sup>33,41</sup>, then the epoxide groups will be consumed in two simultaneous reactions; the first being initiated and catalyzed by the HX molecules, and the second internally catalyzed by the hydroxyl groups in the reaction products. The total rate of consumption of epoxides can therefore be expressed by eqn (2) assuming that homogeneous reaction kinetics are applicable.

$$\frac{d\alpha}{dt} = k_1 C(1-\alpha)(B-\alpha) + K_2 \alpha(1-\alpha)(B-\alpha) \quad (2)$$

where  $\alpha$  is the fraction of epoxide reacted at time  $t$ ,  $C$  is the concentration of the HX molecules,  $B$  is the initial ratio of diamine equivalents to epoxide equivalents ( $B$  equals 1.0 when stoichiometric quantities of the reactants are mixed),  $k_1$  and  $K_2$  are rate constants. If the concentration of HX species is assumed constant, eqn (2) reduces to eqn (3) with  $K_1 = k_1 C$

$$\frac{d\alpha}{dt} = \dot{\alpha} = (K_1 + K_2 \alpha)(1-\alpha)(B-\alpha) \quad (3)$$

The reduced reaction rate,  $\dot{\alpha}_r$ , is defined by eqn (4)

$$\dot{\alpha}_r = \frac{\dot{\alpha}}{(1-\alpha)(B-\alpha)} = K_1 + K_2 \alpha \quad (4)$$

Equation (4) predicts a linear variation of the reduced rate with the extent of cure  $\alpha$ .

## EXPERIMENTAL

### Materials

The epoxy resin systems used in this study consist of a commercial diglycidyl ether of bisphenol A (Dow Chemical Co.; DER 332) and *m*-phenylene diamine (*m*-PDA; Aldrich Chemical Co.; 99% pure). These materials were used as supplied without further purification. The epoxide equivalent weight of the resin was taken as 174 and that of the diamine as 27.

The resin was cured employing stoichiometric and 1.5 times stoichiometric quantities of diamine. The two comonomer mixtures are referred to as EPO-1.0 and EPO-1.5, respectively. The materials were kept in the dark under dry, cold conditions. The comonomer mixture was prepared just prior to use by melting the diamine and the resin separately, then mixing them together and cooling rapidly to room temperature. Caution was taken to avoid overheating the materials during melting.

### *Apparatus and instrumentation*

The thermal and kinetic data were obtained using a Perkin-Elmer DSC-1 differential scanning calorimeter coupled to a General Electric Model 4020 data acquisition and control system computer. An EAI/TR20 analog computer used for integration of the DSC signal was also coupled to the GE computer. Both the DSC and the analog computer signals were displayed on an HP/7100B stripchart recorder. The apparatus was installed in an air-conditioned room maintained at 20°C and 50% relative humidity. Figure 1 shows a block diagram of the experimental arrangement.

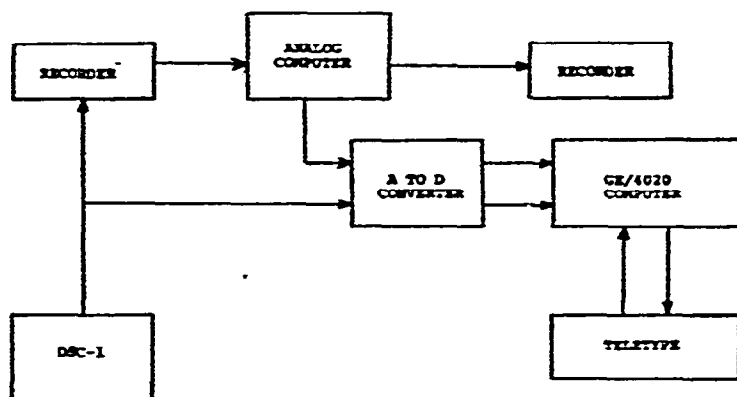


Fig. 1. Block diagram of the experimental arrangement.

The rheological data were obtained using the cone-and-plate geometry of a Rheometrics Mechanical Spectrometer (Model KMS-71C). The conical fixture had an angle of 0.04 radians (2.3°) and the plate diameter was 7.20 cm.

### *DSC calibration*

The DSC was calibrated in the region  $-40$  to  $160^\circ\text{C}$  using the melting points of high purity elements and organic compounds: mercury, indium, stearic acid, *p*-nitrotoluene, naphthalene, benzoic acid and adipic acid (Fisher Thermetric Standards). A predetermined Average Temperature Control setting was chosen, and the indicated melting point for each standard was determined at different heating rates. The indicated melting points at zero heating rate (isothermal calibration) were determined by extrapolation<sup>42</sup>. A temperature correction curve was constructed for each heating rate.

Differential temperature calibration was performed according to the procedure described in the DSC operating manual. An optimum control setting was chosen between the melting points of naphthalene and benzoic acid. The method suggested by Ortiz and Rogers<sup>43</sup> was found useful to obtain an initial adjustment of the Differential Temperature Control setting. The reproducibility of the indicated melting points between successive determinations was found to be better than  $\pm 0.2^\circ\text{C}$ . However, a day-to-day reproducibility was  $\pm 0.3^\circ\text{C}$ . The instrument was kept on continuously under a constant flow of nitrogen through the DSC cell.

### *Isothermal characterization*

To establish a kinetic model for the cure reaction, a set of isothermal cure curves giving the extent of polymerization as a function of time at given temperatures has been obtained first.

Cure isotherms were obtained in the range 320–430 K. Volatile aluminum sample pans were used to reduce losses during heating of the sample in the DSC cell. Weight losses were negligible compared to losses reported by Horie and his co-workers<sup>39</sup> using their modified sample pans. Sample weights were between 12 and 17 mg. High sensitivity ( $2 \text{ mcal sec}^{-1}$ ) was employed at low temperatures.

Actual data collection was initiated and terminated by a computer program which allowed the operator to set the time intervals between data points and accepted input information for data processing. The data were also stored on disc for further use.

A steady isothermal baseline was established at the preset cure temperature using two empty sample pans. The data acquisition system was then initiated, and the sample was introduced into the DSC cell. Thermal equilibrium at the sample and reference holders was achieved in less than 1 min. This was determined from the time required for the recorder pen to return to or override the original isothermal baseline. A time record was obtained of both the rate of heat generation,  $\dot{Q}$ , and the integral heat,  $Q$ . The latter was obtained by integrating the DSC signal with the help of the analog computer. Numerical integration of the DSC signal was also performed by the GE/4020 computer. The reaction was considered complete when the rate curve levelled off to a baseline. The total area under the exotherm curve based on the extrapolated baseline at the end of the reaction gives the isothermal heat of cure referred to later as  $Q_T$ .

On-line processing of the data gives the operator an immediate indication of the reproducibility and goodness of the run. Typical variables, for example the peak value of the reaction rate,  $\dot{Q}_p$ , the cumulative heat generated at the peak,  $Q_p$ , and the total heat,  $Q_T$ , could be printed on the teletype at the end of the run.

In order to obtain a good match between the initial and final isothermal baselines, the radiation characteristics of the sample holders should be perfectly balanced at the cure temperature,  $T_c$ . This was achieved by adjusting the Slope Control setting so that no deflection of the recorder pen was observed when the Range Control setting of the instrument was gradually switched from the "standby" position to the higher sensitivity position of  $2 \text{ mcal sec}^{-1}$ . This procedure was performed before introducing the sample into the DSC cell. Better results were achieved using a dummy fully cured sample instead of an empty sample pan.

After the isothermal cure was completed, the sample was cooled rapidly in the DSC to 320 K. It was then heated at  $5^\circ\text{C min}^{-1}$  to determine its specific heat,  $C_p$ , and the glass transition temperature,  $T_g$ . Each scanning experiment was followed by a blank run to determine the corresponding scanning baseline. The glass transition temperature was defined at the low temperature end of the transition region.

Scanning experiments on uncured samples were carried out at different heating

rates to determine the ultimate heat of cure,  $Q_u$ . The latter was estimated from the area under the scanning exotherm curve with the baseline drawn as a straight line extension of both sides of the scanning exotherm.

### *Rheological characterization*

The viscous behavior of the sample during isothermal cure was followed with time using a Rheometrics mechanical spectrometer as a cone-and-plate viscometer. Details of the experimental procedure are described elsewhere<sup>44</sup>. Viscosity-time isotherms were obtained from the torque-time curve at relatively low shear rate ( $0.25 \text{ sec}^{-1}$ ). As the reaction proceeded, the viscosity increased gradually at first and then sharply indicating gelation and transition into the rubbery region. The temperature of the sample was monitored during the cure and was found to be practically constant.

## RESULTS AND DISCUSSION

### *Isothermal cure data*

Typical DSC isotherm curves for the reaction of DER 332 and *m*-phenylene diamine (*m*-PDA) at different stoichiometric ratios are shown in Figs. 2 and 3. The curves depict an initial reaction rate conforming with the kinetic eqn (2). The existence of a peak in each isothermal cure curve suggests the catalytic effect of the hydroxyl groups present in the reaction products. A sudden decrease or "break" in the rate curve was observed shortly after the peak. This phenomenon was more pronounced at high diamine content with a more abrupt change in the rate. This "break" could be identified with the onset of a diffusion-controlled reaction mechanism due to the increased viscosity of the system<sup>33</sup>. It can also be associated with the gel point and the formation of an infinite network. The levelling of the reaction rate to the original

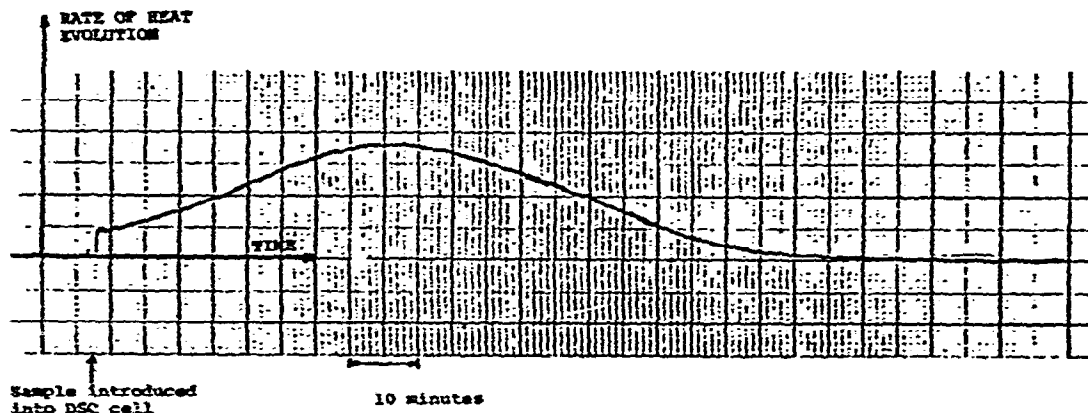


Fig. 2. Typical DSC exotherm curve showing the progress of the isothermal cure reaction of DER 332 epoxy with *m*-phenylene diamine (*m*-PDA) at 355 K. The initial and final isothermal baselines are at identical level.

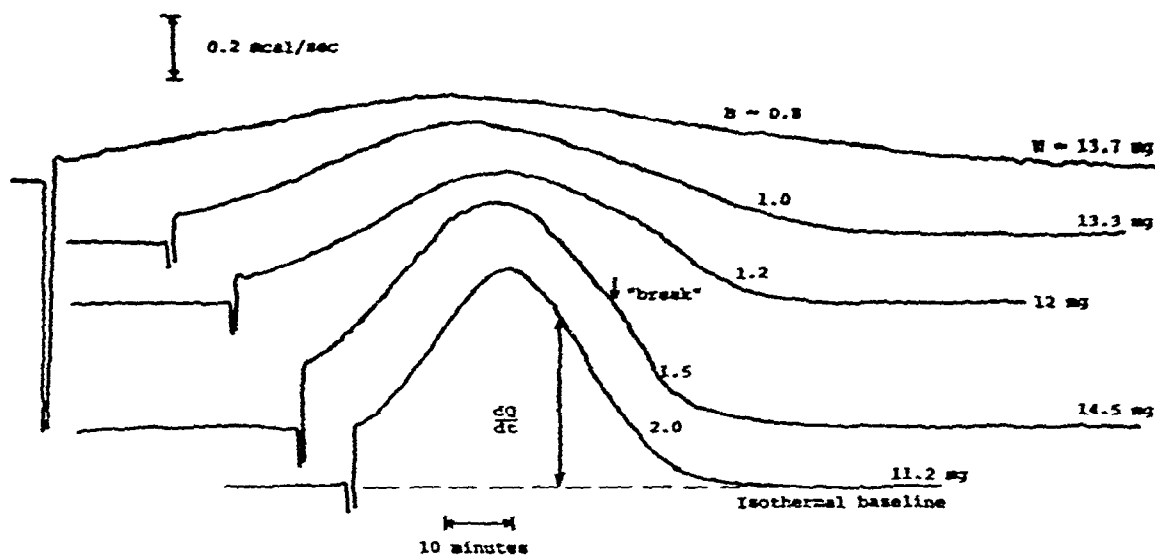


Fig. 3. Typical DSC exotherm curves showing the effect of the stoichiometric *m*-PDA ratio, *B*, on the isothermal cure rate of DER 332 at 355 K, for different sample weights *W*. The "break" in the DSC curve marks the onset of the diffusion-controlled cure.

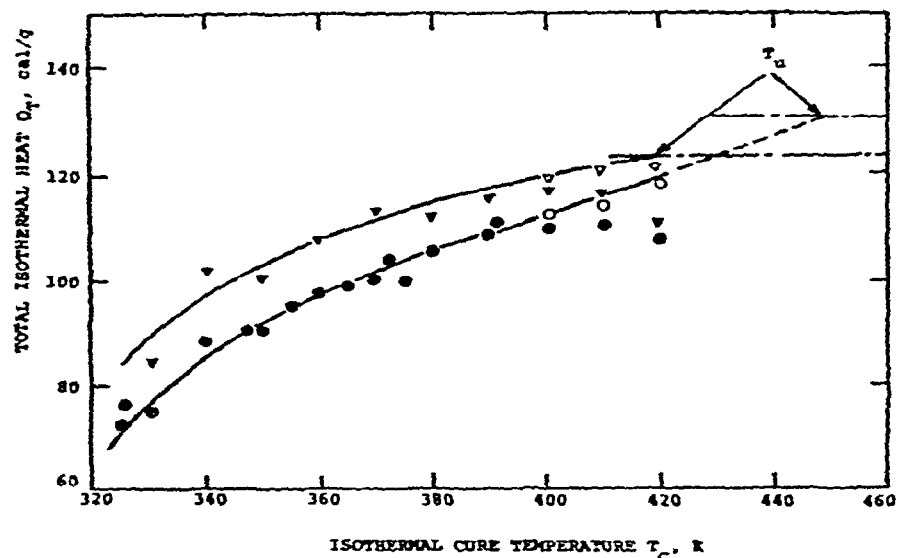


Fig. 4. Total heat of reaction,  $Q_T$ , at different isothermal cure temperatures  $T_c$  for two epoxy/diamine systems. Experimental data: (●) EPO-1.0; (▼) EPO-1.5. Data corrected for the conversion spent during transient heating to  $T_c$ : (○) EPO-1.0; (▽) EPO-1.5.  $T_u$  is the temperature of ultimate cure,  $Q_u$ .

isothermal baseline indicates the cessation of the reaction and the onset of vitrification or glass transition.

Figure 4 shows the variation of the total heat of cure,  $Q_T$ , with the isothermal cure temperature,  $T_c$ , for the two epoxy systems. The cumulative heat generated at the peak of the cure rate isotherm,  $Q_p$ , was found to be practically constant within the range of  $T_c$  studied, as shown in Fig. 5. The measured values of  $Q_T$  at high temperatures are not reliable since the extent of reaction occurring during the transient

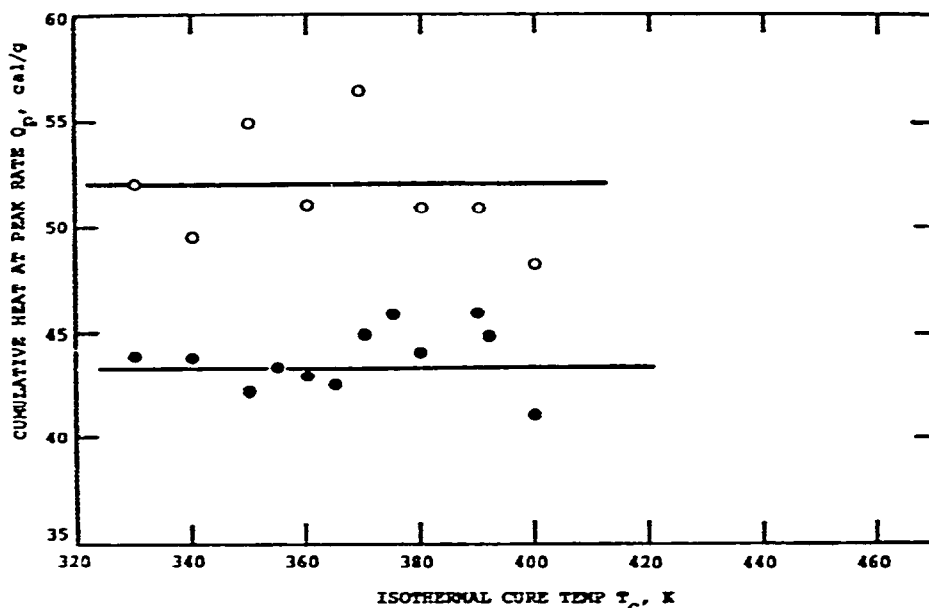


Fig. 5. Cumulative heat generated at the peak,  $Q_p$ , of the DSC isothermal cure rate curve. (●) EPO-1.0; (○) EPO-1.5. Calculated values from eqn (6) are 43.5 and 49 cal  $g^{-1}$ , respectively.

heating of the sample to the desired  $T_c$  in the DSC cell is significant, but is not directly measurable. This would account for the decrease of  $Q_T$  at high temperatures. However, the experimental values of  $Q_T$  at high  $T_c$  can be corrected by integrating the isothermal rate curve from the peak to the completion of the reaction and adding to the result the constant value of  $Q_p$ . Figure 4 shows the corrected data for  $Q_T$  at high temperatures represented by the open symbols.

The ultimate or maximum heat of cure,  $Q_u$ , obtained by scanning the sample from 320 K until no further reaction is evident was found to be  $130 \pm 5$  cal  $g^{-1}$  and  $123 \pm 5$  cal  $g^{-1}$  for EPO-1.0 and EPO-1.5, respectively. Similar values were obtained from isothermal cure data after correcting  $Q_T$  for the transient heating effect at  $T_c > 170^\circ C$  as explained above. The corresponding ultimate molar heat of cure was calculated to be approximately 26 kcal  $mol^{-1}$  of epoxide reacted, assuming complete consumption of the epoxides by the amines. The data are in good agreement with the results of Klute and Viehmann<sup>45</sup> ( $26 \pm 0.7$  kcal  $mol^{-1}$ ) and those of Horie<sup>33</sup> ( $24.5 \pm 0.6$  kcal  $mol^{-1}$ ) for similar epoxy/amine systems.



Extrapolation of the data in Fig. 4 to  $Q_u$ , yields a value of 178°C for the ultimate isothermal cure temperature,  $T_u$ , of EPO-1.0. This compares well with the value of 180°C reported by Gillham<sup>25</sup> from dynamic mechanical measurements on an identical epoxy/diamine formulation under isothermal conditions using torsional braid analysis (TBA).

The residual extent of cure defined as  $(Q_u - Q_T)/Q_u$ , decreases exponentially with increasing cure temperature in the range 320 to 390 K. Figure 6 shows a linear correlation of the data on a semi-logarithmic plot for EPO-1.0. Similar results were

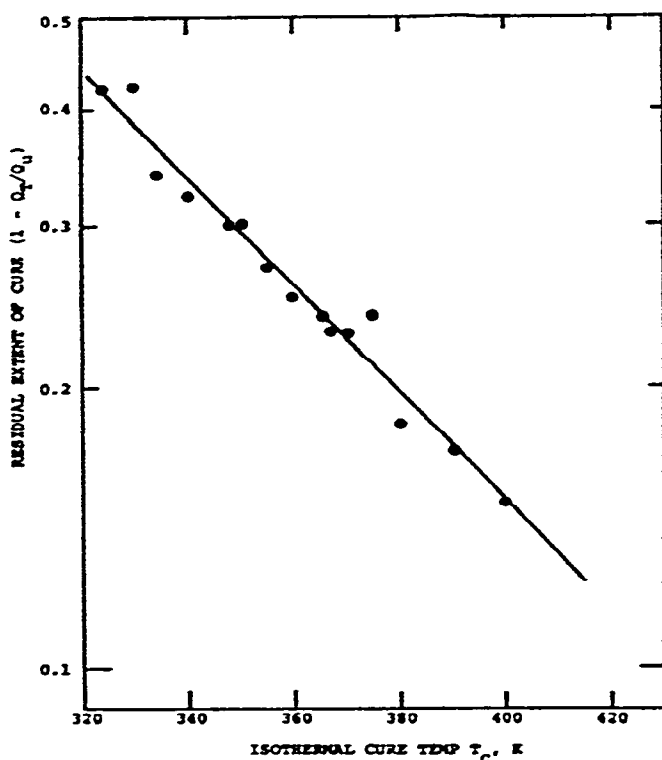


Fig. 6. Dependence of the residual extent of cure on isothermal cure temperature for EPO-1.0.

obtained for EPO-1.5. Assuming that the correlation holds at low temperature, extrapolation of the data to a residual extent of cure of 1.0 gives an estimate of the critical temperature  $T_0$  below which no significant reaction occurs. From Fig. 6,  $T_0$  for EPO-1.0 was calculated at  $-15^\circ\text{C}$ . Horie<sup>33</sup> reported a value of  $-14^\circ\text{C}$  for the glass temperature of a similar system at zero crosslinking density.

#### *Kinetic model and activation energies*

The kinetic model represented by eqn (3) is somewhat different from the models employed by a variety of workers<sup>10,35,36</sup>, which are usually based on  $n$ th order kinetics. Such models are not satisfactory because they do not predict the peak

observed in the isothermal rate of reaction curve or the sigmoidal shape of the heat of reaction curve. Furthermore, an  $n$ th order equation cannot realistically describe the progress of the entire reaction because of the different transitions (gelation, vitrification) the material undergoes during cure.

At first, it is necessary to check the validity of the kinetic model in eqn (4). Typical plots of the reduced reaction rate,  $\hat{\alpha}_r$ , versus the extent of cure,  $\alpha$ , are shown in Figs. 7 and 8. The reduced reaction rate increases linearly with conversion during the initial stages of cure as predicted by eqn (4). However, deviation from linearity marked by a sharp decrease in the reduced rate is observed at a conversion that could be related to the onset of a diffusion-controlled reaction mechanism. This conversion was found to correspond to the time at which the "break" in the DSC cure isotherms occurred, as depicted in Fig. 3. Beyond that critical conversion, which increases with the isothermal cure temperature, the rate constants  $K_1$  and  $K_2$  become strong functions of the diffusion rate of the reactants<sup>33</sup> and, consequently, of the extent of reaction. The dependence of the rate constants on temperature and mass diffusivities for diffusion-controlled second order reactions has been described by the Rabinowitch equation<sup>46</sup> which reduces to the well-known Arrhenius expression for homogeneous reactions. It may be worth mentioning that the peak in the reduced rate curves does not necessarily correspond to the peak in the DSC rate isotherms.

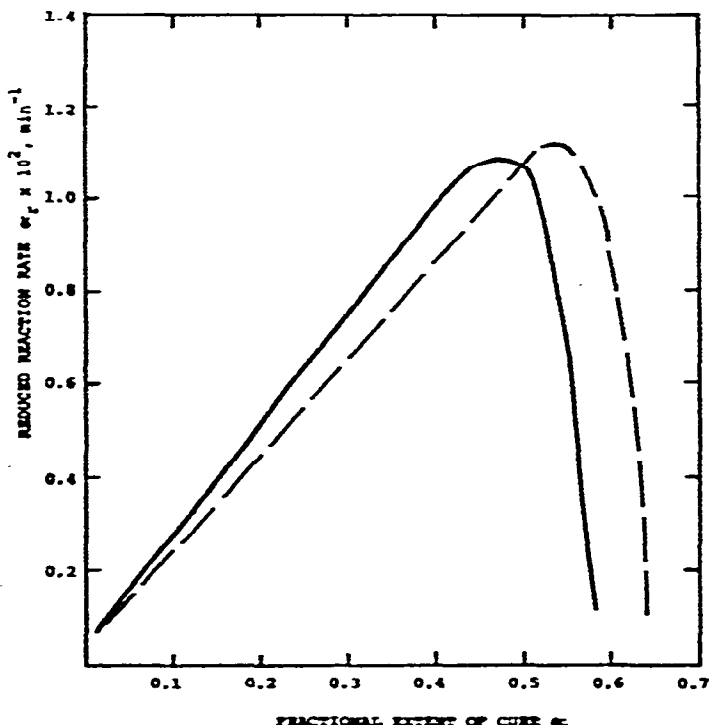


Fig. 7. Variation of the reduced isothermal cure rate,  $\hat{\alpha}_r$ , defined by eqn (4) with the fractional extent of epoxide conversion,  $\alpha$ , at 330 K. (—) EPO-1.0; (---) EPO-1.5.

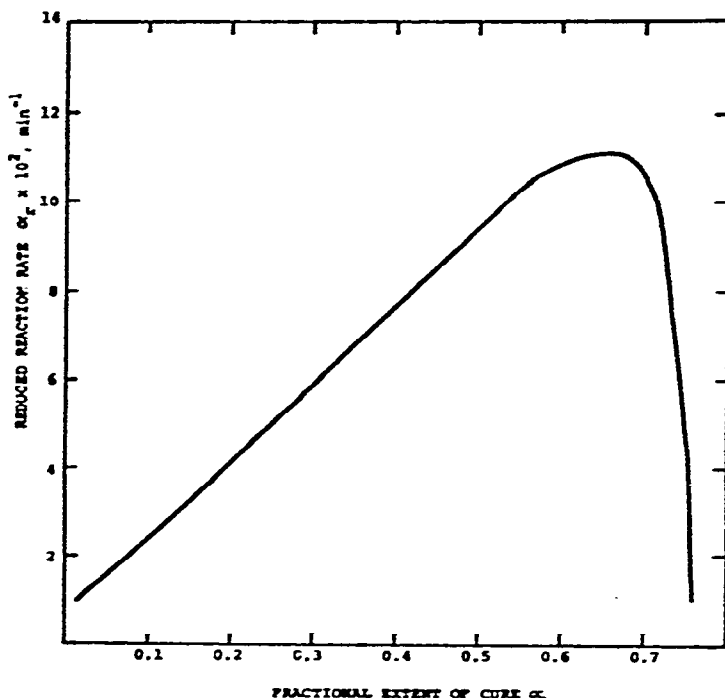


Fig. 8. Variation of the reduced isothermal cure rate,  $\dot{\alpha}_r$ , with the extent of cure,  $\alpha$ , for EPO-1.0 at 375 K.

Equation (4) was fitted to the linear segment of the reduced isotherms using a weighted least-square technique. An arbitrary weighting factor of 0.9 was used for the data points at the two ends of the line segment. The constants  $K_1$  and  $K_2$  were found to correlate with temperature according to an Arrhenius equation as shown in Figs. 9 and 10. Correlation coefficients lie between 0.987 and 0.999. The Arrhenius constants are listed in Table 1 for the two systems. The activation energies are in good agreement with values reported in the literature<sup>33</sup>. As expected, the activation energy for the autocatalytic reaction (11 kcal mol<sup>-1</sup>) is less than for the normal reaction (19–21 kcal mol<sup>-1</sup>).

Comparison between typical experimental DSC data and the results predicted by the model is shown graphically in Figs. 11 and 12 for both epoxy systems. As expected, good agreement (within  $\pm 5\%$ ) is obtained for the initial stage of reaction. The model, however, predicts higher reaction rates for the later stages of the cure reaction since the diffusion of the reactants and the dependence of the rate constants on the extent of cure were not accounted for in the model. These contribute to the fast decay of the reaction rate whereas the model assumes a finite value.

The results in Table 1 show that  $K_1$  may be ignored compared with  $K_2\alpha$  for large value of  $\alpha$ . Hence eqn (3) can be approximated by eqn (5)

$$\frac{d\alpha}{dt} = \dot{\alpha} \approx K_2\alpha(1-\alpha)(B-\alpha) \quad (5)$$

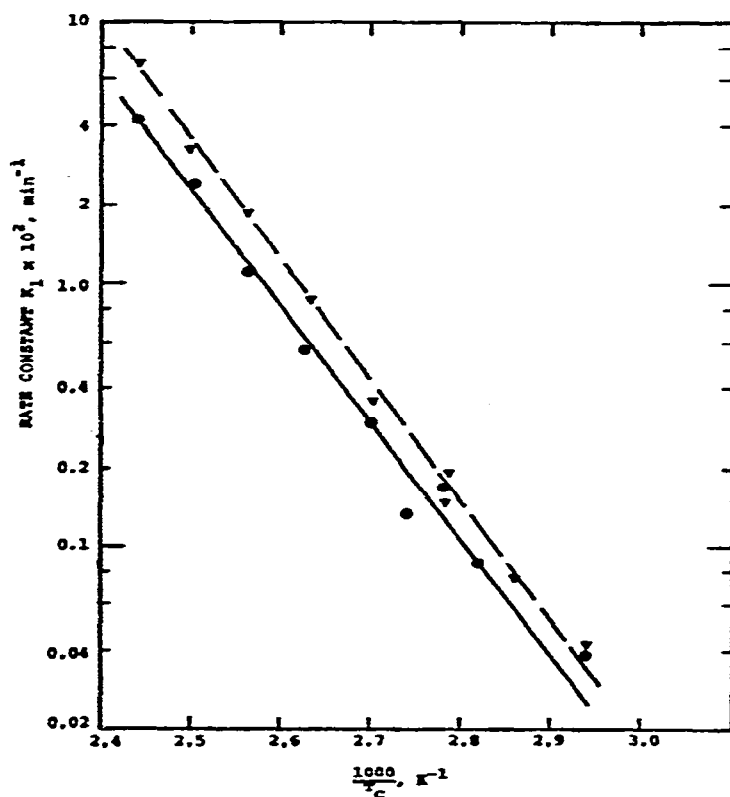


Fig. 9. Arrhenius plot of the rate constant  $K_1$  in eq (3); (●) EPO-1.0; (▼) EPO-1.5.

TABLE I  
KINFTIC AND THERMODYNAMIC PARAMETERS FOR EPOXY CURE

Parameter	EPO-1.0	EPO-1.5
$K_1$ ( $\text{min}^{-1}$ )	$5.53 \times 10^8 \exp(-19.4 \text{ kcal mol}^{-1}/RT)$	$9.65 \times 10^9 \exp(-21.1 \text{ kcal mol}^{-1}/RT)$
$K_2$ ( $\text{min}^{-1}$ )	$8.06 \times 10^5 \exp(-11.4 \text{ kcal mol}^{-1}/RT)$	$3.7 \times 10^5 \exp(-11.0 \text{ kcal mol}^{-1}/RT)$
$Q_D$ ( $\text{cal g}^{-1} \text{min}^{-1}$ )	$5.94 \times 10^7 \exp(-12.4 \text{ kcal mol}^{-1}/RT)$	$5.38 \times 10^7 \exp(-11.9 \text{ kcal mol}^{-1}/RT)$
$t_g$ (min)	$1.0 \times 10^{-6} \exp(12.8 \text{ kcal mol}^{-1}/RT)$	$1.0 \times 10^{-6} \exp(12.5 \text{ kcal mol}^{-1}/RT)$
$Q_p$ ( $\text{cal g}^{-1}$ )	43	52
$Q_u$ ( $\text{cal g}^{-1}$ )	130	123
$Q_g$ ( $\text{cal g}^{-1}$ )	75	86
$T_{22}$ ( $^{\circ}\text{C}$ )	69	75
$T_{g\infty}$ ( $^{\circ}\text{C}$ )	158	122
$T_{c2}$ ( $^{\circ}\text{C}$ )	56	63
$T_u$ ( $^{\circ}\text{C}$ )	178	147
$\alpha_x$	0.58	0.70

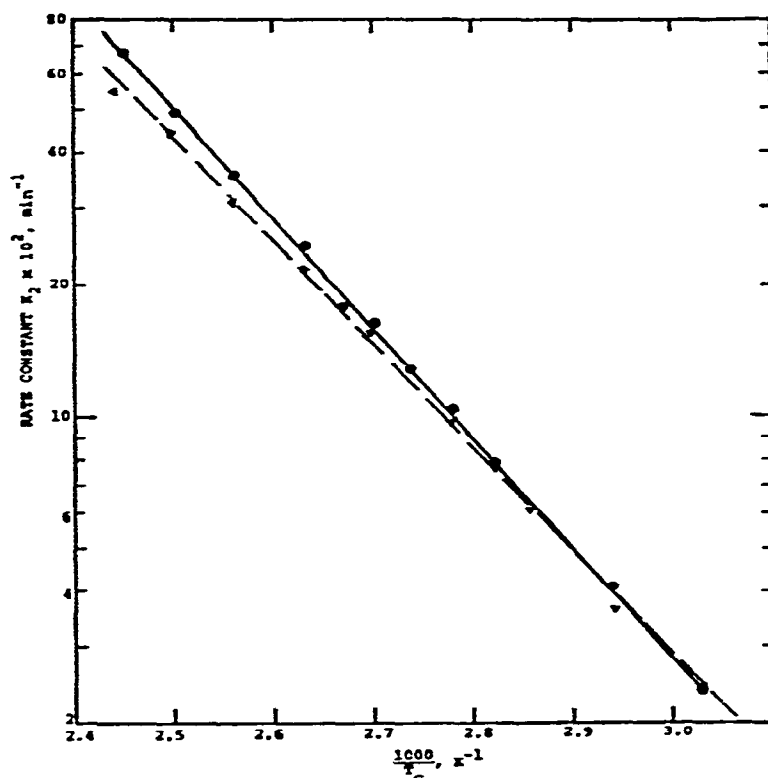


Fig. 10. Arrhenius plot of the rate constant  $K_2$  in eqn (3); (●) EPO-1.0; (▼) EPO-1.5.

At the peak of the reaction rate isotherm  $(d^2\alpha/dt^2)_{\text{peak}} = 0$ . Thus, from eqn (5) the following approximate relation is obtained:

$$3\alpha_p^2 - 2\alpha_p(1+B) + B \approx 0 \quad (6)$$

where  $\alpha_p$  is the extent of reaction at the peak rate and is equal to  $Q_p/Q_u$ . Values of  $\alpha_p$  from eqn (6) are 0.35 and 0.39 for EPO-1.0 and EPO-1.5, respectively, independent of temperature.

Figure 13 is an Arrhenius plot of the peak isothermal reaction rate,  $\dot{Q}_p$ . The data fit a straight line with a correlation coefficient of 0.998. The Arrhenius constants determined by least-squares fitting are listed in Table 1. The values of activation energy are comparable with those obtained for the rate constant  $K_2$ . This is consistent with eqn (5) yielding a direct proportionality of  $\dot{Q}_p$  and  $K_2$ . Therefore,  $\dot{Q}_p$  can be considered as a kinetic parameter to determine an overall apparent activation energy.

### Gel point measurements

In any system in the process of forming a three-dimensional polymer network, the extent of reaction at the gel point is an intrinsic property of the system and is not a function of the experimental conditions. According to the Flory-Stockmayer theory for step-growth polymerization, the extent of reaction at the gel point,  $\alpha_g$ , for both

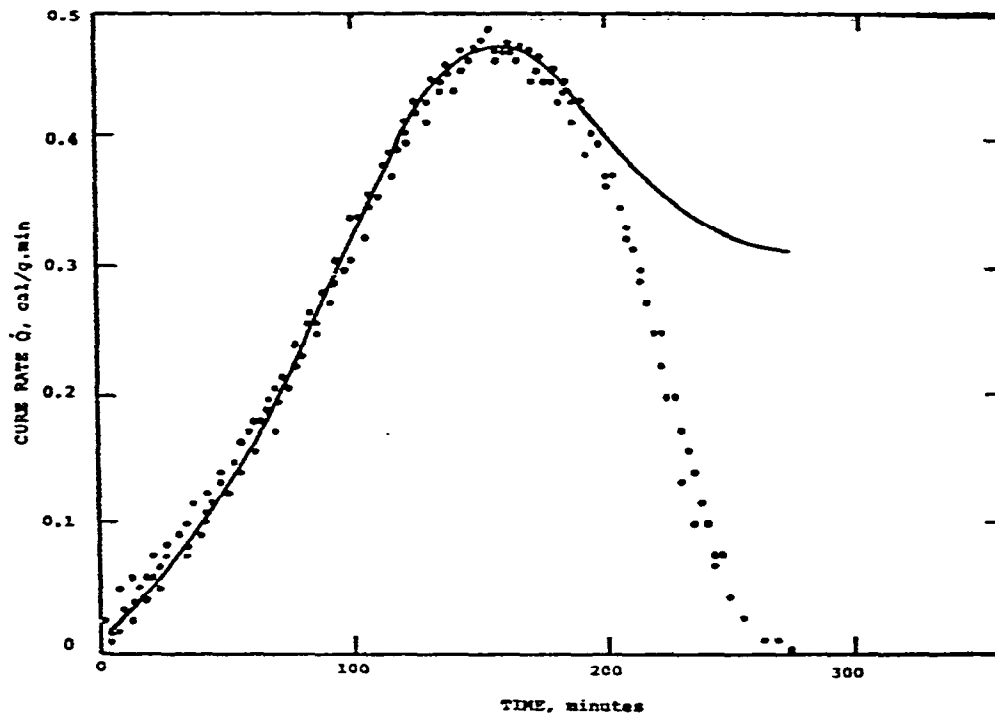


Fig. 11. Comparison between experimental (●) and calculated (—) isothermal cure rate for EPO-1.0 at 330 K using the model of eqn (3).

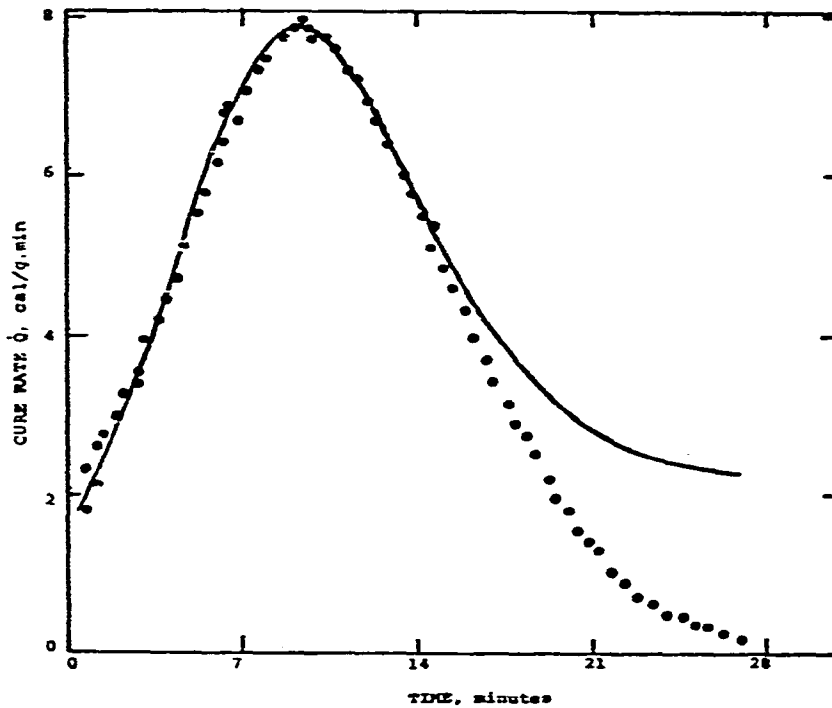


Fig. 12. Comparison between experimental (●) and calculated (—) isothermal cure rate for EPO-1.5 at 380 K using the model of eqn (3).

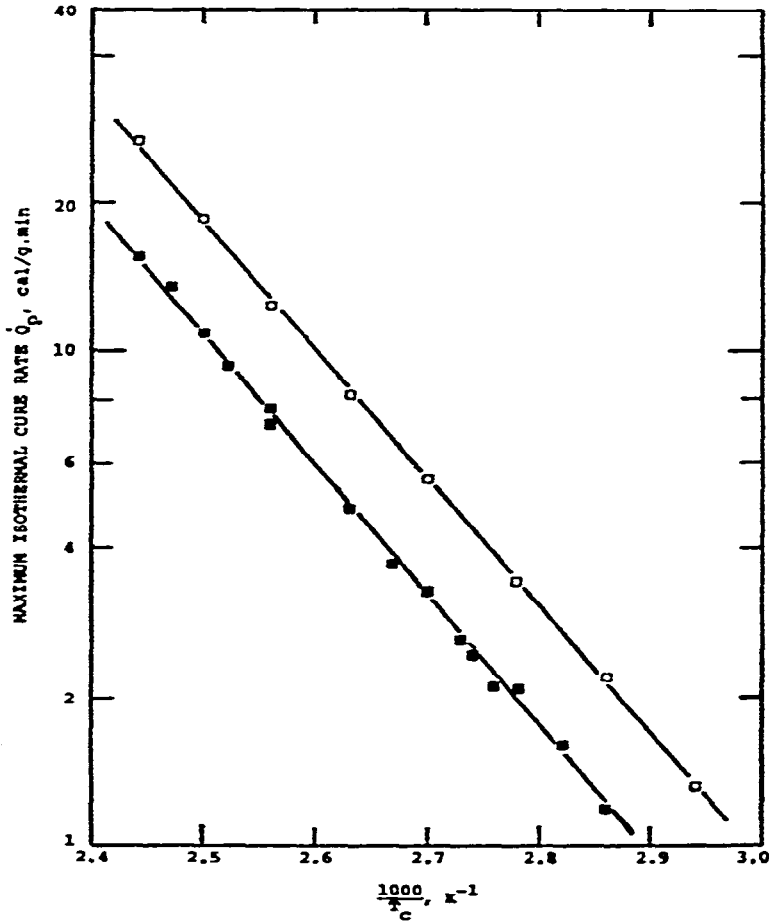


Fig. 13. Arrhenius plot of the peak isothermal cure rate. (■) EPO-1.0; (□) EPO-1.5.

EPO-1.0 and EPO-1.5 systems was calculated to be 58% and 70%, respectively. The corresponding values for the cumulative exothermic heat of cure,  $Q_g$ , are  $75 \pm 2$  and  $86 \pm 2$  cal g<sup>-1</sup> for EPO-1.0 and EPO-1.5, respectively.

If it is assumed that  $K_1 \ll K_2 \alpha$  near the gel point, then integration of eqn (5) yields an equation of this functional form

$$F(\alpha_g) = K_2 t_g = \text{constant}$$

where  $t_g$  is the time required for the material to reach the onset of gelation. Hence,  $t_g$  would have the same Arrhenius temperature dependence as  $K_2$ , and can therefore be used as a kinetic variable for determining an overall activation energy for the process of crosslinking.

Figure 14 shows a typical Arrhenius plot of the rheologically-determined gel time,  $(t_g)_{\text{rheo.}}$ , and the kinetic gel time,  $(t_g)_{\text{kin.}}$ . The latter was determined from the kinetic model as the time required to reach a conversion  $\alpha_g$  during an isothermal cure at  $T_c$ . The rheological gel time was identified with the time required for the epoxy

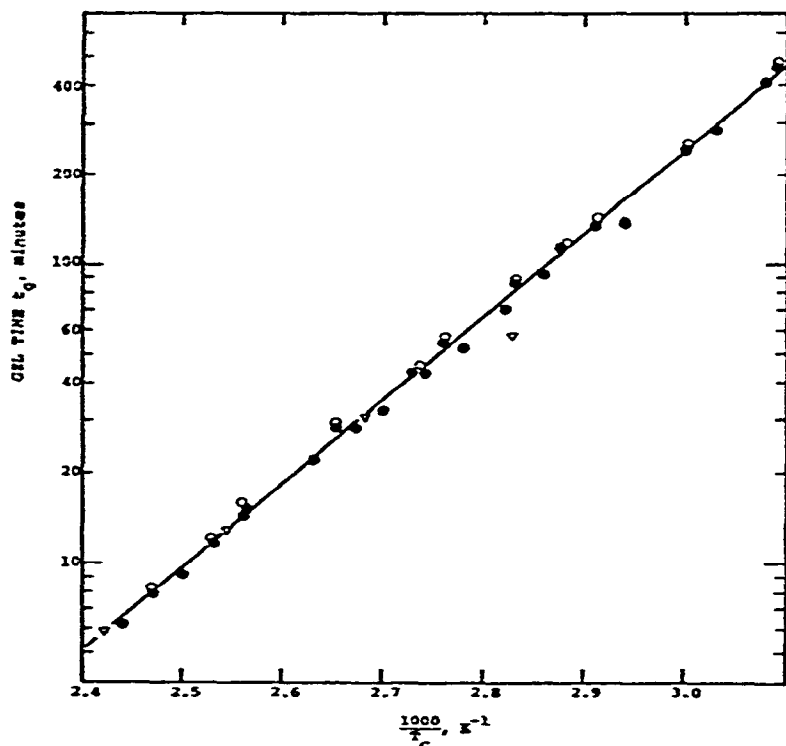


Fig. 14. Arrhenius plot of gel time for EPO-1.0 during isothermal cure at  $T_c$ , (●) kinetic gel time from DSC; (○) rheological gel time from viscosity measurements; (∇) mechanical gel time from TBA (ref. 25).

sample to reach a viscosity equal to  $10^5$  poises under isothermal cure conditions. The good agreement between the two types of gel time supports the validity and consistency of the kinetic model over the temperature range studied. Thus, the rheological gel time could be a useful kinetic parameter particularly at low temperatures where calorimetric measurements are not sufficiently sensitive to provide kinetic information on the cure reactions. The data agree with reported values of gel time using dynamic mechanical techniques<sup>33</sup>. The Arrhenius constants for the gel time-temperature correlation are shown in Table 1. Correlation coefficients are 0.998–0.999.

The activation energies reported in Table 1 are generally in very good agreement with published data for similar epoxy systems. Typical values: 14–16 kcal mol<sup>-1</sup> reported by Gough and Smith<sup>21</sup>, and Kil<sup>18</sup>, from gel time measurements; 10–12 kcal mol<sup>-1</sup> reported by Jenkins and Karre<sup>17</sup>, and Gillham<sup>25</sup> from infrared and dynamic mechanical techniques; 12–14 kcal mol<sup>-1</sup> reported by Prime<sup>36</sup>, and Horie<sup>33</sup> from reaction rate measurements (DSC), and Aukward, Warfield and Petrie<sup>8</sup>, and Miller<sup>9</sup> from electrical resistivity measurements.

#### Glass transition and specific heat

The glass temperature  $T_g$  is an additional measure of the extent of crosslinking



and increases throughout curing, i.e.,  $T_g(t)$ . As soon as  $T_g$  equals or exceeds  $T_c$  by a certain value, the reaction terminates irrespective of the continuation of the isothermal treatment. The system "freezes chemically". The data in Fig. 15 show that the glass temperature approaches a value which is always 10 to 13°C higher than the temperature at which the curing was carried out. That difference disappears near the

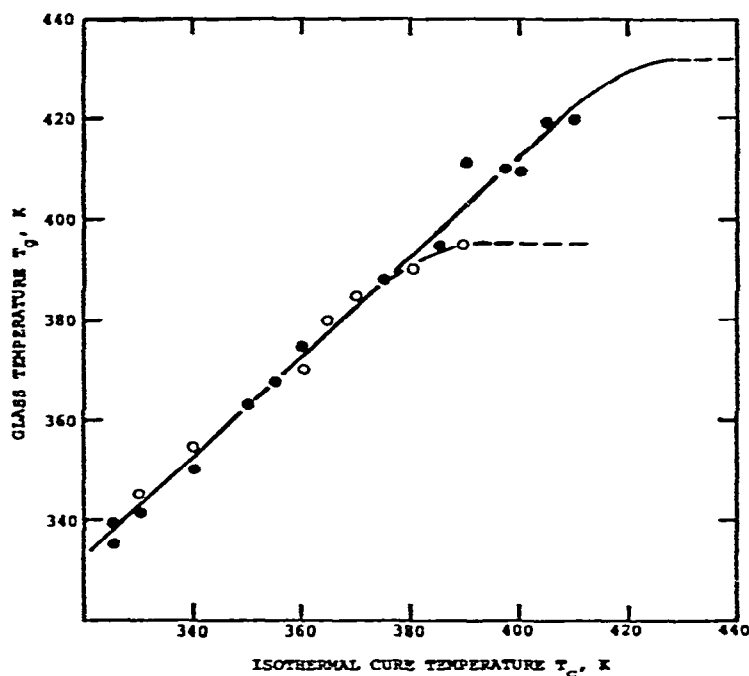


Fig. 15. Variation of glass temperature with the isothermal cure temperature. (●) EPO-1.0; (○) EPO-1.5.

glass temperature of the fully cured material,  $T_{g\infty}$ . Values of  $T_{g\infty}$  are listed in Table 1. The above observations are consistent with the results reported in the literature<sup>12,17,25</sup> from dynamic mechanical techniques (TBA, vibrating reed). If  $Q_T$  is equal to  $Q_g$ , and the corresponding isothermal cure temperature is  $T_{cg}$ , then the processes of vitrification and gelation occur simultaneously. If  $T_c$  exceeds  $T_{cg}$ , the system will pass through gelation first and then through vitrification<sup>25</sup>. At  $T_c < T_{cg}$  the system undergoes vitrification only since gelation occurs at a constant conversion independent of temperature. The glass temperature at the gel point,  $T_{gg}$ , is found from Fig. 15 and is listed in Table 1.

The data of Figs. 6 and 15 suggest a logarithmic relationship between the extent of cure and the glass temperature. Shibayama<sup>47</sup> proposed a similar relationship for the increase in glass temperature with crosslinking density.

It was also found that the arithmetic product of  $T_g$  and the specific heat change due to vitrification,  $(\Delta C_p T_g)$ , is practically constant. Results for EPO-1.0 gave a value

of  $32 \pm 3 \text{ cal g}^{-1}$ . This agrees with the value of  $30 \pm 2 \text{ cal g}^{-1}$  reported by Boyer<sup>48</sup> for different polymers in the range 330–430 K.

#### CONCLUSION

Differential scanning calorimetry (DSC) can be successfully used over a wide temperature range to obtain isothermal cure data for epoxy polymers. A simple mechanistic kinetic model describing the initial stages of cure of epoxy/diamine systems was found to be consistent with DSC and rheological data. The model is not valid for the later stages of cure where the reaction mechanism is diffusion-controlled. Agreement of the model with experimental isothermal cure data is within  $\pm 5\%$ . The model yields activation energy values which agree well with those obtained from rheological and dynamic measurements. The activation energy was found not to be affected significantly by the presence of excess diamine. The time for the material to gel under isothermal conditions, and the peak isothermal reaction rate can be used as kinetic variables to determine an overall activation energy. The overall predominant internally catalyzed reaction is considered to be third order (one each in epoxy, amine, and hydroxyl concentrations) until the onset of the diffusion-controlled reaction rate. The residual extent of cure was found to vary exponentially with the isothermal cure temperature and the glass transition temperature. The latter was found to exceed the cure temperature by approximately 10 to 13°C. A critical isothermal cure temperature, where the processes of vitrification and gelation occur simultaneously, can be determined from DSC cure data and the gelation theory. Maximum cure can be achieved by curing the material isothermally above the ultimate cure temperature.

#### ACKNOWLEDGEMENTS

The authors wish to thank Mr. M. Ryan of McGill University for obtaining the experimental rheological data, and the Dow Chemical of Canada for supplying the materials used in this study. Financial support from the National Research Council of Canada, the Ministry of Education of the Province of Quebec and McGill University is gratefully acknowledged.

#### REFERENCES

- 1 H. W. Mackinney and J. T. Spalik, *SPE Trans.*, 5 (1965) 39.
- 2 J. Feltzin, D. M. Longenecker and I. Petker, *SPE Trans.*, 5 (1965) 111.
- 3 R. W. Warfield and M. C. Petrie, *J. Polym. Sci.*, 37 (1959) 305.
- 4 D. E. Kline, *J. Appl. Polym. Sci.*, 4 (1960) 123.
- 5 A. F. Lewis and J. K. Gillham, *J. Appl. Polym. Sci.*, 6 (1962) 422.
- 6 A. F. Lewis, *SPE Trans.*, 3 (1963) 201.
- 7 H. Dannenberg, *SPE J.*, 15 (1959) 875.
- 8 J. A. Aukward, R. W. Warfield and M. C. Petrie, *J. Polym. Sci.*, 27 (1958) 199.
- 9 B. Miller, *J. Appl. Polym. Sci.*, 10 (1966) 217.
- 10 M. A. Acitelli, R. B. Prime and E. Sacher, *Polymer*, 12 (1971) 335.

- 11 V. Adamec, *J. Polym. Sci.*, A-1, 10 (1972) 1277.
- 12 W. Fisch, W. Hofmann and R. Schmid, *J. Appl. Polym. Sci.*, 13 (1969) 295.
- 13 R. E. Cuthrell, *J. Appl. Polym. Sci.*, 12 (1968) 955.
- 14 Y. Tanaka and H. Kakiuchi, *J. Appl. Polym. Sci.*, 7 (1963) 1951.
- 15 P. N. Son and C. D. Weber, *J. Appl. Polym. Sci.*, 17 (1973) 2415.
- 16 L. Shechter, J. Wynstra and R. P. Kurkijy, *Ind. Eng. Chem.*, 48 (1956) 94.
- 17 R. Jenkins and L. Karre, *J. Appl. Polym. Sci.*, 10 (1966) 303.
- 18 T. A. Kil, A. I. Aksenov and G. S. Kitukhina, *Sov. Plast.*, 3 (1972) 16.
- 19 M. R. Kamal, S. Sourour and M. Ryan, *SPE Technical Papers*, 19 (1973) 187.
- 20 I. T. Smith, *Polymer*, 2 (1961) 95.
- 21 L. J. Gough and I. T. Smith, *J. Appl. Polym. Sci.*, 3 (1960) 362.
- 22 R. P. White, Jr., *SPE Technical Papers*, 19 (1973) 192.
- 23 K. M. Hollands and J. L. Kalnin, *Advances in Chemistry Series*, Vols. 92 and 60, ACS, Washington 1970.
- 24 T. Kakurai and T. Noguchi, *Kobunshi Kagaku*, 19 (1962) 546.
- 25 P. G. Babayevsky and J. K. Gillham, *J. Appl. Polym. Sci.*, 17 (1973) 2067.
- 26 B. N. Komarov and I. M. Al'shits, *Sov. Plast.*, 1 (1973) 75.
- 27 T. K. Kwei, *J. Polym. Sci.*, A-2, 4 (1966) 943.
- 28 A. S. Kenyon and L. E. Nilsen, *J. Macromol. Sci., Chem.*, A3 (2) (1969) 275.
- 29 R. G. C. Arridge and J. H. Speake, *Polymer*, 13 (1972) 443.
- 30 A. F. Lewis, *SPE Trans.*, 3 (1963) 201.
- 31 R. P. Kneoling and D. E. Kline, *J. Appl. Polym. Sci.*, 13 (1969) 2411.
- 32 R. A. Fava, *Polymer (London)*, 9 (1968) 137.
- 33 K. Horie, H. Hiura, M. Sawada, I. Mita and H. Kambe, *J. Polym. Sci.*, A-1, 8 (1970) 1357.
- 34 O. R. Abolafia, *SPE Technical Papers*, 15 (1969) 610.
- 35 R. B. Prime and E. Sacher, *Polymer (London)*, 13 (1972) 455.
- 36 R. B. Prime, *Polym. Eng. Sci.*, 13 (1973) 365.
- 37 H. J. Borchardt and F. Daniels, *J. Am. Chem. Soc.*, 79 (1957) 41.
- 38 H. E. Kissinger, *Anal. Chem.*, 29 (1957) 1702.
- 39 K. Horie, I. Mita and H. Kambe, *J. Polym. Sci.*, A-1, 7 (1969) 2561; 6 (1968) 2663; 8 (1970) 2839.
- 40 V. D. Moiseev, et al., *Sov. Plast.*, 8 (1973) 69.
- 41 J. F. Harrod, *J. Appl. Polym. Sci.*, 6 (1962) S63.
- 42 S. Strella and P. F. Erhardt, *J. Appl. Polym. Sci.*, 13 (1969) 1373.
- 43 L. W. Ortiz and R. N. Rogers, *Thermochim. Acta*, 3 (1972) 383.
- 44 M. R. Ryan, *Rheology of Polyester and Epoxy Liquids During Cure*, M. Eng. Thesis, McGill University, Montreal, 1973.
- 45 C. H. Klute and W. Viehmann, *J. Appl. Polym. Sci.*, 5 (1961) 86.
- 46 E. Rabinowitch, *Trans. Faraday Soc.*, 33 (1937) 1225.
- 47 K. Shibayama, *Kobunshi Kagaku*, 18 (1961) 181.
- 48 R. F. Boye, *J. Macromol. Sci. Phys.*, B7 (1973) 487.